

Durham Research Online

Deposited in DRO:

04 December 2018

Version of attached file:

Accepted Version

Peer-review status of attached file:

Peer-reviewed

Citation for published item:

Li, Y. and Zhang, S. and Hobbs, R. and Caiado, C. and Sproson, A.D. and Selby, D. and Rooney, A.D. (2019) 'Monte Carlo sampling for error propagation in linear regression and applications in isochron geochronology.', Science bulletin., 64 (3). pp. 189-197.

Further information on publisher's website:

<https://doi.org/10.1016/j.scib.2018.12.019>

Publisher's copyright statement:

© 2018 This manuscript version is made available under the CC-BY-NC-ND 4.0 license
<http://creativecommons.org/licenses/by-nc-nd/4.0/>

Additional information:

Use policy

The full-text may be used and/or reproduced, and given to third parties in any format or medium, without prior permission or charge, for personal research or study, educational, or not-for-profit purposes provided that:

- a full bibliographic reference is made to the original source
- a [link](#) is made to the metadata record in DRO
- the full-text is not changed in any way

The full-text must not be sold in any format or medium without the formal permission of the copyright holders.

Please consult the [full DRO policy](#) for further details.

Monte Carlo sampling for error propagation in linear regression and applications in isochron geochronology

Yang Li^{1,2,3}, Shuang Zhang³, Richard Hobbs², Camila Caiado⁴, Adam D. Sproson^{2,5}, David Selby², Alan D. Rooney³

¹State Key Laboratory of Lithospheric Evolution, Institute of Geology and Geophysics, Chinese Academy of Sciences, Beijing, 10029, China

²Department of Earth Sciences, Durham University, Durham, DH1 3LE, UK

³Department of Geology and Geophysics, Yale University, New Haven, Connecticut, 06511, USA

⁴Department of Mathematical Sciences, Durham University, Durham, DH1 3LE, UK

⁵Atmosphere and Ocean Research Institute, The University of Tokyo, 5-1-5 Kashiwa-no-ha, Kashiwa 275-8564, Japan

Corresponding author: Yang Li (geoliy@mail.iggcas.ac.cn; cugliyang@126.com)

Key points:

- Full propagation of uncertainties from experimental sources and underlying assumptions in linear regression and their implications in isochron dating;
- An ability to incorporate geological information;

Abstract

Geochronology is essential for understanding Earth's history. The availability of precise and accurate isotopic data is increasing; hence it is crucial to develop transparent and accessible data reduction techniques and tools to transform raw mass spectrometry data into robust chronological data. Here we present a Monte Carlo sampling approach to fully propagate uncertainties from linear regressions for isochron dating. Our new approach makes no prior assumption about the causes of variability in the derived chronological results and propagates uncertainties from both experimental measurements (analytical uncertainties) and underlying assumptions (model uncertainties) into the final age determination. Using synthetic examples, we find that although the estimates of the slope and y-intercept (hence age and initial isotopic ratios) are comparable between the Monte Carlo method and the benchmark "Isoplot" algorithm, uncertainties from the later could be underestimated by up to 60%, which are likely due to an incomplete propagation of model uncertainties. An additional advantage of the new method is its ability to integrate with geological information to yield refined chronological constraints. The new method presented here is specifically designed to fully propagate errors in linear regressions especially in geochronological applications involves linear regressions such as Rb-Sr, Sm-Nd, Re-Os, Pt-Os, Lu-Hf, U-Pb (with discordant points), Pb-Pb and Ar-Ar.

Keywords

Linear regression; Isochron; Geochronology; Uncertainty Propagation; Monte Carlo; Isoplot

1
2
3 38 **1. Introduction**
4
5

6 39 Geochronology is an essential aspect of Earth sciences, and advances in this field have
7
8 40 resulted in many breakthroughs in understanding the history of our solar system and the
9
10 41 evolution of life on Earth [1]. In general, extracting geologically meaningful ages from rocks
11
12 42 and minerals starts with sample collection, followed by sample processing, and isotopic ratio
13
14 43 measurements via mass spectrometry. The raw isotopic ratios generated by mass spectrometers
15
16 44 then need to be transformed into atomic ratios, and eventually into chronological dates with
17
18 45 propagation of associated uncertainties [e.g., 2, 3]. Over the past three decades, a great number
19
20 46 of analytical innovations and instrumentation advances have emerged, which gave rise to
21
22 47 unprecedented levels of accuracy and precision for isotopic ratio measurements as well as
23
24 48 pioneering new radiometric systems for questions ranging from early solar system evolution to
25
26 49 Anthropocene climate change. Advances in the precision and accuracy as well as the expansion
27
28 50 of available geochronometers has been facilitated by a combination (often iteratively) of better
29
30 51 analytical approaches and robust, transparent and accessible data reduction tools [e.g., 4, 5-13].
31
32
33 52 To more fully harness these technical improvements, it is critical to concomitantly develop
34
35 53 data reduction techniques and appropriate visualization methods. Although there have been
36
37 54 significant progresses made in data reduction techniques for U-Th-Pb and Ar-Ar systems [3,
38
39 55 6, 7, 14-20], fewer advances have been seen in isochron dating, a method utilized for systems
40
41 56 including Re-Os.
42
43
44
45
46

47 57 Isochron dating is based on linear regression in which one determines the slope, y-
48
49 58 intercept and associated uncertainties of the best fitting line to the parent and daughter isotopic
50
51 59 ratios (including their uncertainties and error correlations). The fundamental assumptions
52
53 60 behind isochron dating include: (1) all co-genetic samples have near-identical initial daughter
54
55 61 isotopic compositions; (2) samples begin accumulating daughter isotopes via radiogenic decay
56
57 62 at the same time; (3) these samples remain closed in terms of both parent and daughter isotopes
58
59
60

following the accumulation of the daughter isotope. A further requirement is that these samples should have variable parent isotope (or daughter isotope) ratios to define a line. This linear regression is routinely carried out by the “Isoplot” program that is based on a Microsoft Excel macro [2, 21] and includes York’s algorithm [22-24]. This algorithm performs a least-squares fit to data with normally distributed but correlated uncertainties, and assumes that the data points lie along a straight line (isochron) and offsets from this line are due to imperfect measurements, otherwise known as analytical uncertainties. In reality however, the data points might not fall on a straight line even if they could be measured perfectly because of differences in initial isotopic composition, varying ages and/or open system behavior, which we will refer as model uncertainties. To address this, the “Isoplot” program uses two different techniques (additional options are discussed below) for error propagation and decides which one to use based on the probability of how well the data “fits” to the line. If the probability of fit is satisfactory, “Isoplot” assumes that analytical uncertainty is the only cause of scatter and uses York’s algorithm to propagate only analytical uncertainties to produce a so-called Model 1 age. If the fit of the data to a common line is not satisfactory resulting in a violation of York’s assumption (i.e., in the case of over-dispersion), “Isoplot” uses an adapted regression that accounts for an unknown but normally distributed variation in the initial isotopic ratios of the samples [2, 25], producing a Model 3 age. Though the users can choose the cutoff value between the two Models (between 0.05 and 0.3 with a default of 0.15), in the absence of additional geologic constraints, there is no standard criteria to choose this cutoff value, which can lead to inconsistencies in chronological results if this value is not properly documented.

“Isoplot” also offers a Model 2 solution in which case equal weights and zero error correlations are assigned to the samples, as opposed to those used in Model 1 and Model 3 where each sample has a weighting proportional to the inverse square of its analytical uncertainties (also accounts the error correlation). When the assumption that residuals

1
2
3 88 (observed scatter) of the data-points from a straight line have a normal (Gaussian) distribution
4
5 89 is invalid, “Isoplot” has an option called “Robust regression” which makes no assumptions
6
7
8 90 about the cause(s) of the observed scatter of the data from a straight line. We do not discuss
9
10 91 these two options further as they are rarely used and beyond the scope of this study.

11
12 92 As pointed out by Ludwig [26], uncertainty determined by Monte Carlo sampling is the
13
14 93 most reliable approach, therefore in this paper we propose an method to determine the slope,
15
16 94 y-intercept and their uncertainties, based on Monte Carlo sampling and simple linear regression.
17
18 95 Unlike the Monte Carlo method in York et al., (2004) [24], the proposed method here
19
20 96 propagates not only analytical uncertainties, but also uncertainties arising from the underlying
21
22 97 assumptions (model uncertainties). This approach differs from Model 1 and Model 3 solutions
23
24 98 from Isoplot as our new method propagates uncertainties in a consistent manner regardless of
25
26 99 the probability of fit and hence avoids subjective choosing of the cut-off value discussed above.
27
28
29
30
31 100 Our method can be applied to data with any goodness of fit and distinguishes between
32
33 101 analytical and model uncertainties. This paper discusses three key aspects: (1) the Monte Carlo
34
35 102 based method; (2) the examination of differences and similarities to Isoplot; and (3) the use of
36
37 103 a synthetic dataset to demonstrate the potential to integrate independent geological information
38
39 104 for refined chronologic constraints.

40
41
42
43 105 **2. Monte Carlo simulation**

44
45
46 106 **2.1 Experimental data and their uncertainties**

47
48
49 107 The parent and daughter isotopic ratios (X, Y) of a sample are measured experimentally,
50
51 108 with their uncertainties (δX , δY) inherited from the analytical procedure. Additionally, the
52
53 109 uncertainties of the parent and daughter isotopic ratios are typically correlated due to the
54
55 110 utilization of a common isotope used to convert absolute atomic numbers into isotopic ratios
56
57 111 (e.g., ^{86}Sr in $^{87}\text{Rb}/^{86}\text{Sr}$ and $^{87}\text{Sr}/^{86}\text{Sr}$; ^{144}Nd in $^{147}\text{Sm}/^{144}\text{Nd}$ and $^{143}\text{Nd}/^{144}\text{Nd}$), which is quantified

by a correlation coefficient [denoted by ρ or ρ ; 27]. Experimental data with the same parent and daughter isotopic ratios and uncertainties, but variable error correlations are graphically illustrated in **Figure 1A** as error ellipses at the 2-sigma level (all uncertainties are presented at the 2-sigma level in absolute values unless otherwise stated). By definition, a high error correlation indicates that the sources of δX and δY are predominately from one contributor, which for isotope geochemistry is likely to be caused by the analytical uncertainty of the stable isotope used to convert absolute atomic numbers into isotopic ratios. As emphasized by Ludwig [26] and illustrated in **Figure 1A**, the 2-sigma ellipses including error correlation extend farther than the 2-sigma range of δX and δY , which is a non-intuitive characteristic of joint distributions. As such, excluding error correlations for linear regressions will yield an incorrect uncertainty for the slope and its uncertainty [28]. Hence it is critical to report and use accurate error correlations for the experimental data in all geochronological studies which can be estimated through differentiation and observation [2]. The analytical uncertainties with error correlation can also be presented as probability density functions (PDFs, **Fig. 1B**). This probability density function is the basis for the resampling process used in our Monte Carlo method.

2.2 Propagation of analytical uncertainties

We demonstrate the principles of our Monte Carlo based technique using a synthetic example consisting of five samples. The parent and daughter isotopic ratios and associated uncertainties including error correlations of the five samples are graphically illustrated in **Figure 2A** as error ellipses. To propagate analytical uncertainties, we perform the following steps:

1. for each of the five samples, we randomly select a coordinate from its corresponding probability density function as that defined in **Figure 1B**. Each

1
2
3
4
5
6
7
8
9
10
11
12
13
14
15
16
17
18
19
20
21
22
23
24
25
26
27
28
29
30
31
32
33
34
35
36
37
38
39
40
41
42
43
44
45
46
47
48
49
50
51
52
53
54
55
56
57
58
59
60

sampled coordinate is considered to be a pair of absolute values without uncertainty (Fig. 2A);

2. once a coordinate has been selected for each of the five samples, the parameters (slope and y-intercept) of the regression line are determined (Fig. 2A) following a least-square estimation [29]. The slope and y-intercept of this regression line is plotted in Figure 2B;

3. repeating steps 1 and 2 yields a distribution representing the probability of slope and y-intercept of the five samples. By increasing the iteration times (Figs. 2C and 2E), the shape of the resulting probability distribution becomes apparent (Figs. 2D and 2F). We acknowledge here that more iterations will yield a more accurate distribution, but will also increase computing time. A discussion on how to balance the iteration time and computing resource is presented in section 2.4 below.

This approach only propagates analytical uncertainties but not uncertainties from the linear regression itself. This is illustrated by the example in Figure 3. For a dataset consisting of five samples that have no analytical uncertainty and do not plot on a common line (Fig. 3A), using the above algorithm will result in no uncertainty for the slope and y-intercept (Fig. 3B), which is not a plausible result because the fitted line does not pass through all the five samples. We term these non-analytical uncertainties as the model uncertainty. The primary contributors of this model uncertainty include differences in the initial isotope composition, ages, or those which arise from open isotopic system behavior violating the fundamental assumptions behind isochron dating. In realistic scenarios it is likely that both analytical and model uncertainties will be present at some level though careful selection of samples and refined measurements maybe used to minimize their effect. Using the simple Monte Carlo algorithm described above which only propagates analytical uncertainties and fails to capture this extra source of

161 uncertainty. We therefore propose an extension of our method to account for this as described
162 below.

163 2.3 Propagation of model uncertainties

164 Uncertainties for the slope and y-intercept of the regression line in each sampling step
165 in section 2.2 (Fig. 2) are calculated as standard errors following that of James et al., (2009)
166 [29]. Further, these uncertainties are correlated as defined by the correlation coefficient (C) in
167 equation 1,

$$168 \quad C = - \sum_{i=1}^n (x_i) / (n \times (\sum_{i=1}^n (x_i^2))^{0.5}) \quad (\text{equation 1})$$

169 where n is the number of samples (e.g., 5 for the example in Fig. 2), and x_i denotes the sampled
170 point's X-axis.

171 Knowing these uncertainties and error correlation for each sampling step, it is possible
172 to include them by replacing the outcome of each sampling step by a new probability density
173 distribution. This process is illustrated in Figure 3, where one of the outcomes from the
174 sampling step (Fig. 3B) is replaced by a new probability density distribution (Figs. 3D). For
175 input data with analytical uncertainties (Figs. 3E), when model uncertainties are included for
176 all simulations, a final distribution (blue in Fig. 3F) is obtained. This final distribution includes
177 both analytical and model uncertainties, and we term them as total uncertainties. In the presence
178 of both analytical uncertainties and model uncertainties, we cannot determine exactly whether
179 the scatter in the final distribution is inherited from analytical uncertainties or caused by model
180 uncertainties, or a combination of both.

181 Statistical analysis is applied to the final distribution to quantify the uncertainties for
182 data interpretation. We use the means and two standard deviations of the slope and y-intercept,
183 plus the correlation between them, to assess the significance of this final distribution.
184 Additionally, the contribution of analytical uncertainties to the total uncertainties (analytical +
185 model uncertainties) could be assessed. Here we emphasize that as discussed above, analytical

uncertainties could be an additional source of model uncertainties, hence the contribution only can be assessed semi-quantitatively.

The advantage of this method is that regardless of the degree of fit, both analytical and model uncertainties are propagated into the final distribution. In other words, the degree of fit is not a prerequisite to alter the strategy of error propagation. As such, the proposed method ensures that quoted uncertainties can be fairly compared as they are calculated in a consistent manner.

2.4 The iteration times

To achieve a representative final distribution for the given sample set, a high number of iterations are required at the expense of consuming more computing resources and time. In this regard, the iteration times should be balanced between the accuracy of the final distribution and the simulation time. Here we monitor the mean and standard deviation of the final distribution and stop iteration once this mean and standard deviation are stabilized. Our preliminary experiment suggests that an iteration count of about 10^6 is sufficient in most cases, and could be increased when necessary.

3. Comparison with Isoplot

It is important to compare the results from the Monte Carlo based approach with those from the Isoplot program to understand differences in the assumptions and how they propagate into the resultant age estimations. In the following section, we construct a synthetic experimental data set to highlight the magnitude of these differences and explore implications in isochron dating.

3.1 Synthetic experimental dataset

Using the Re-Os isotopic system as an example, where ^{187}Re decays to ^{187}Os with a decay constant of $1.666 \times 10^{-11} \text{ year}^{-1}$ [30, 31], we generate synthetic examples for the

experiment (Table 1). To be representative of geological scenarios, the examples are designed to cover plausible scenarios in isochron dating, as represented by the probability of fit which varies between 0 and 1 (Figure 4). For uncertainty propagation using the Isoplot program, we follow the default approach in the Isoplot program to set the cut-off value as 0.15. As can be seen from the following discussion, using different cut-off values should not bias our conclusion. Below we outline the approaches generating these examples.

1. An age and an initial daughter isotopic ratio (i.e., $^{187}\text{Os}/^{188}\text{Os}_{\text{initial}}$) are randomly assigned between 100 and 4500 Ma and 0.2–1.2, respectively, following uniform distributions.
2. The number of samples, n , used to construct an isochron is randomly chosen between 5 and 30 following a uniform distribution.
3. For the n samples, their parent isotopic ratios (i.e., $^{187}\text{Re}/^{188}\text{Os}$) at present day are randomly selected following uniform distributions between 100 and 1000. Specifically, for each example, we first randomly pick a lowest ratio and a highest ratio which lie between 100 and 1000. Afterwards, we randomly pick $n-2$ ratios following a uniform distribution between that lowest ratio and highest ratio. The purpose of this specific approach is to guarantee that for these examples, the variety of the parent isotopic ratios (spread of the isochron) in each example follows a uniform distribution.
4. The daughter isotopic ratios (e.g., $^{187}\text{Os}/^{188}\text{Os}$) at present day of the n samples are calculated individually following equation 2 using the t , initial daughter isotopic ratio and parent isotope ratios generated in step 1, 2 and 3, respectively.

$$^{187}\text{Os}/^{188}\text{Os} = ^{187}\text{Os}/^{188}\text{Os}_{\text{initial}} + ^{187}\text{Re}/^{188}\text{Os} * (e^{\lambda t} - 1) \quad (\text{equation 2})$$
5. We then introduce scatter to the daughter isotopic ratios by adding or subtracting a value ranging from 0.2 to 1.2 % of the corresponding daughter

1
2
3 235 isotopic ratios following uniform distributions, and the decision whether to add
4
5 236 or subtract is also random. Note that this scatter serves to imitate model
6
7
8 237 uncertainties. The model uncertainties are introduced through modifying the
9
10 238 daughter isotopic ratios, which cover all the potential causes of model
11
12 239 uncertainties including variations in initial isotopic composition and age, as well
13
14
15 240 as open system behaviour to the isotopic system and imperfect measurements.
16
17 241 6. The 2-sigma relative uncertainty (i.e., percentage uncertainty) of the parent and
18
19 242 daughter isotope ratios are randomly assigned between 0.2 and 1 % following
20
21 243 uniform distributions, with their error correlations randomly given between 0.4
22
23
24 244 and 0.999, which also follow uniform distributions.

25
26 245 The data generated above are processed by our new Monte Carlo method as well as the
27
28 246 Isoplot program. Therefore, one age and one initial isotopic composition plus their associated
29
30
31 247 uncertainties (2-sigma) will be obtained from the Isoplot program either following Model 1 (p
32
33 248 > 0.15) or Model 3 ($0 < p < 0.15$) solutions. For the Monte Carlo simulation, one age, one
34
35 249 initial isotopic ratio, and associated total uncertainties (analytical uncertainties+ model
36
37
38 250 uncertainties) are obtained for each example. We perform this process 10000 times, and as
39
40 251 expected, the probability of these examples varies between 0 and 1 with the corresponding
41
42 252 Mean Square Weighted Deviation (MSWD) ranging from >10 to 0.

43
44
45 253 3.2. Results from Monte Carlo method and the Isoplot program

46
47
48 254 Regardless of which linear regression tool is employed, the slopes and y-intercepts,
49
50 255 hence ages and initial isotopic ratios, are the same (Figs. 4A-D). Minimal scatter exists when
51
52 256 the spread in the synthetic data points is limited, which renders an accurate age estimation
53
54
55 257 difficult. Notably, uncertainties obtained from the Monte Carlo simulation are consistently
56
57 258 larger than those from the Isoplot program (Figs. 4E-5F). Here we use the $R_{MC/Iso}$ to illustrate
58
59 259 these results, where $R_{MC/Iso}$ equals to age uncertainties (total) from the Monte Carlo method

divided by age uncertainties from the Isoplot program. When p decreases from 1 to 0.15, the running mean of $R_{MC/Iso}$ increases from 2 to 2.5, and indicates a progressively increasing degree of underestimation of uncertainties by the Isoplot program. When p decreases from 0.15 to 0, we observe a significant decrease in the running mean of the $R_{MC/Iso}$ from ~ 2 to ~ 1.5 , and then gradually decrease to >1 . This relationship can further be illustrated by plotting $R_{MC/Iso}$ as a function of MSWD (which is dependent on p , Fig. 4F), and shows that $R_{MC/Iso}$ reduce from 2.5 to 1.5 as the MSWD increases from 1.3 to 2.5, ultimately $R_{MC/Iso}$ approaches one when the scatter is sufficiently large (i.e., $MSWD \gg 2.5$). A notable feature here is the abrupt change in the relationship between $R_{MC/Iso}$ and probability/MSWD when p approaches 0.15. Such an abrupt transition is mainly due to the contrasting error propagation strategies in Isoplot caused by the utilization of an arbitrary cut-off value.

These results indicate that uncertainties following the Model 1 scenarios in the Isoplot program are underestimated by 50 – 60 % compared to total uncertainties derived from the Monte Carlo method (as calculated by the difference between the uncertainties relative to the Monte Carlo based total uncertainties). For the Model 3 age in Isoplot, the uncertainties can also be underestimated by as much as 60 %, though uncertainties become more comparable for increasing MSWD.

An underestimation of uncertainty could be detrimental in geological studies when high temporal resolution is essential. For example, when verifying the relationship between two geological processes that are indistinguishable in time (e.g., 1000 ± 0.6 Ma and 999 ± 0.6 Ma), an underestimation of the uncertainties by 50 % will yield ages of 1000 ± 0.3 Ma and 999 ± 0.3 Ma, which could lead to a conclusion that the two geological events were not contemporaneous in time, hence rejecting a direct causal link between them. In contrast, with full propagation of the uncertainties, a potential causal link cannot be ruled out.

1
2
3
4
5
6
7
8
9
10
11
12
13
14
15
16
17
18
19
20
21
22
23
24
25
26
27
28
29
30
31
32
33
34
35
36
37
38
39
40
41
42
43
44
45
46
47
48
49
50
51
52
53
54
55
56
57
58
59
60

We speculate that the underestimation of uncertainties in the Model 1 ages arises from only considering analytical uncertainties without incorporating model uncertainties. This is supported by the observations that the analytical-only uncertainties from the Monte Carlo based method are comparable (though slightly larger, discussed below) to those from the Model 1 scenario in Isoplot program (Fig. 4G-H). The underestimation of uncertainties in the Model 3 ages is less transparent, but most likely due to an incomplete propagation of model uncertainties.

A further feature is that when $p > 0.15$, the analytical only uncertainties from our Monte Carlo method are slightly larger than those from the Model 1 solution (Figs. 4G and 4H). Such a discrepancy is expected based on York et al., (2004) [24] — the uncertainties from Monte Carlo method only becomes comparable with those from the least square method when sampling the least-squares-adjusted data points (i.e., the projection of the observed data point onto the isochron) by Monte Carlo, rather than sampling the observed data points as has been done here.

4. Potential to integrate geological information

An additional advantage of using the Monte Carlo based method is that the resulting distribution of age and initial isotopic ratios can be adjusted to integrate with geological information and produce improved chronological constraints. We demonstrate this by using a synthetic example consisting of 12 samples. Their $^{187}\text{Re}/^{188}\text{Os}$ and $^{187}\text{Os}/^{188}\text{Os}$ ratios and associated uncertainties including error correlations (Table 2) are used to determine their age and initial isotopic ratio. Results obtained from the Monte Carlo method and the algorithm of the Isoplot program are presented in Figure 5. The ages and initial isotopic ratios from the two methods are essentially the same (Isoplot age = 540 ± 2 Ma, initial $^{187}\text{Os}/^{188}\text{Os} = 0.600 \pm 0.013$; Monte Carlo age = 540 ± 6 , initial $^{187}\text{Os}/^{188}\text{Os} = 0.600 \pm 0.063$), but uncertainties from the Isoplot program are significantly smaller as discussed above. If there is evidence that these

samples are younger than 541 Ma, i.e., based on independent geological constraints, it is reasonable to discard regression results that are older than 541 Ma from the final distribution (Fig. 5). By doing so, the final distribution is altered, and skewed to younger ages and higher initial isotopic ratios (Fig. 6). If we consider quantiles to interpret uncertainties for this distribution, the age estimate changes to 539^{+2}_{-6} Ma and the initial isotopic composition to $0.616^{+0.026}_{-0.035}$ at the 95% percentile level. Similarly, if the initial isotopic ratio can be independently constrained, this information can also be integrated into the Monte Carlo method. This approach is analogous to a common practice in isochron dating, where a sample or a mineral containing low or negligible parent isotope is selected together with samples bearing high parent isotope for isochron dating (e.g., using matrix and garnet with low and high $^{176}\text{Lu}/^{177}\text{Hf}$ ratios, respectively for Lu-Hf dating; using plagioclase and pyroxene with low and high $^{147}\text{Sm}/^{144}\text{Nd}$ ratios, respectively for Sm-Nd dating), through which the y-intercept of the isochron is “fixed” by the sample (e.g., matrix and plagioclase) plotting near or at the y-intercept. It is possible that the independent constrained geological information would also have uncertainties or follow a certain distribution, these also can be considered in our Monte Carlo method.

In addition, with semi-quantitatively constrained contributions of analytical uncertainties to the total uncertainties, the new method provides guidance on how to yield refined chronological constrains. For example, if the uncertainties are dominated by analytical approaches, then improving experimental techniques would be an obvious next step to generate improved chronological information. In contrast, if analytical uncertainty is not the primary contributor to the total uncertainty, then the studied samples may not meet the criteria for isochron dating, and better sampling strategy would be the solution for refined chronological constrains.

5. Conclusions

A Monte Carlo based method is developed to estimate parameters (slope, y-intercept) in linear regression with full propagation of their uncertainties, which is then applied to data reduction for isochron geochronology. Crucially, the new method propagates both analytical and model uncertainties in a consistent manner, and also allows for the user to employ *a posteriori* geological criterion to yield refined chronological constrains and interpret the significance of the analytical/model uncertainty. Using a synthetic data set, results obtained from the Monte Carlo method and those from the Isoplot program are compared. The comparison indicates that although the estimates of the slope (age) and y-intercept (initial isotopic ratio) from both methods are similar, uncertainties following the Model 1 approach in the Isoplot program are underestimated by ~60 %. For Model 3 solution in the Isoplot program, the uncertainties can be underestimated by as much as 60 % depending on the goodness of fit, and the results from the two methods only start to converge when the goodness of fit approaches 0 (i.e., MSWD >> 2.5). We further demonstrate that geological information can be integrated into our Monte Carlo based method to yield improved chronological constraints.

Acknowledgements

YL acknowledges the NERC Numerical Earth Science Modelling courses at Durham University for developing coding skills, especially the help from Jeroen van Hunen and Dimitrios Michelioudakis. The research is partially funded by a grant (SKL-K201706) from the State Key Laboratory of Lithospheric Evolution, Institute of Geology and Geophysics, Chinese Academy of Sciences. DS acknowledges the TOTAL endowment fund. ADR and YL acknowledges generous funding from Yale University. The code associating this manuscript is available from www.github.com/xxx.

356 **References**

- 357 1. Harrison, T. M., Baldwin, S. L., Caffee, M., et al., *It's About Time: Opportunities and*
358 *Challenges for US Geochronology*. Institute of Geophysics and Planetary Physics
359 Publication, 2015. **6539**: p. 56.
- 360 2. Ludwig, K. R., *User's manual for Isoplot 3.00: a geochronological toolkit for Microsoft*
361 *Excel*. 2003.
- 362 3. Schmitz, M. D. Schoene, B., *Derivation of isotope ratios, errors, and error correlations*
363 *for U-Pb geochronology using ^{205}Pb - ^{235}U -(^{233}U)-spiked isotope dilution thermal*
364 *ionization mass spectrometric data*. *Geochemistry, Geophysics, Geosystems*, 2007.
365 **8**(8): p. n/a-n/a.
- 366 4. Mattinson, J. M., *Zircon U-Pb chemical abrasion ("CA-TIMS") method: Combined*
367 *annealing and multi-step partial dissolution analysis for improved precision and*
368 *accuracy of zircon ages*. *Chemical Geology*, 2005. **220**(1-2): p. 47-66.
- 369 5. McLean, N. M., Condon, D. J., Schoene, B., et al., *Evaluating uncertainties in the*
370 *calibration of isotopic reference materials and multi-element isotopic tracers*
371 *(EARTHTIME Tracer Calibration Part II)*. *Geochimica Et Cosmochimica Acta*, 2015.
372 **164**: p. 481-501.
- 373 6. Renne, P. R., Mundil, R., Balco, G., et al., *Joint determination of ^{40}K decay constants*
374 *and $^{40}\text{Ar}^*/^{40}\text{K}$ for the Fish Canyon sanidine standard, and improved accuracy for*
375 *$^{40}\text{Ar}/^{39}\text{Ar}$ geochronology*. *Geochimica et Cosmochimica Acta*, 2010. **74**(18): p. 5349-
376 5367.
- 377 7. Rivera, T. A., Storey, M., Zeeden, C., et al., *A refined astronomically calibrated*
378 *$^{40}\text{Ar}/^{39}\text{Ar}$ age for Fish Canyon sanidine*. *Earth and Planetary Science Letters*, 2011.
379 **311**(3): p. 420-426.
- 380 8. Creaser, R. A., Papanastassiou, D. A. Wasserburg, G. J., *Negative Thermal Ion Mass-*
381 *Spectrometry of Osmium, Rhenium, and Iridium*. *Geochimica Et Cosmochimica Acta*,
382 1991. **55**(1): p. 397-401.
- 383 9. Völkening, J., Walczyk, T. Heumann, K. G., *Osmium isotope ratio determinations by*
384 *negative thermal ionization mass spectrometry*. *International Journal of Mass*
385 *Spectrometry and Ion Processes*, 1991. **105**: p. 147-159.
- 386 10. Jicha, B. R., Singer, B. S. Sobol, P., *Re-evaluation of the ages of $^{40}\text{Ar}/^{39}\text{Ar}$ sanidine*
387 *standards and supereruptions in the western U.S. using a Noblesse multi-collector mass*
388 *spectrometer*. *Chemical Geology*, 2016. **431**: p. 54-66.
- 389 11. Condon, D. J., Schoene, B., McLean, N. M., et al., *Metrology and traceability of U-Pb*
390 *isotope dilution geochronology (EARTHTIME Tracer Calibration Part I)*. *Geochimica*
391 *Et Cosmochimica Acta*, 2015. **164**: p. 464-480.
- 392 12. Li, X. H. Li, Q. L., *Major advances in microbeam analytical techniques and their*
393 *applications in Earth Science*. *Science Bulletin*, 2016. **61**(23): p. 1785-1787.
- 394 13. Chen, S., Wang, X., Niu, Y., et al., *Simple and cost-effective methods for precise*
395 *analysis of trace element abundances in geological materials with ICP-MS*. *Science*
396 *Bulletin*, 2017. **62**(4): p. 277-289.
- 397 14. McLean, N. M., Bowring, J. F. Bowring, S. A., *An algorithm for U-Pb isotope dilution*
398 *data reduction and uncertainty propagation*. *Geochemistry Geophysics Geosystems*,
399 2011. **12**: p. n/a-n/a.
- 400 15. McLean, N. M., Bowring, J. F. Gehrels, G., *Algorithms and software for U-Pb*
401 *geochronology by LA-ICPMS*. *Geochemistry Geophysics Geosystems*, 2016. **17**(7): p.
402 2480-2496.

16. Bowring, J. F., McLean, N. M. Bowring, S. A., *Engineering cyber infrastructure for U-Pb geochronology: Tripoli and U-Pb_Redux*. Geochemistry, Geophysics, Geosystems, 2011. **12**.
17. Horstwood, M. S. A., Kosler, J., Gehrels, G., et al., *Community-Derived Standards for LA-ICP-MS U-(Th-)Pb Geochronology - Uncertainty Propagation, Age Interpretation and Data Reporting*. Geostandards and Geoanalytical Research, 2016. **40**(3): p. 311-332.
18. Vermeesch, P., *Revised error propagation of Ar-40/Ar-39 data, including covariances*. Geochimica Et Cosmochimica Acta, 2015. **171**: p. 325-337.
19. Dutton, A., Rubin, K., McLean, N., et al., *Data reporting standards for publication of U-series data for geochronology and timescale assessment in the earth sciences*. Quaternary Geochronology, 2017. **39**: p. 142-149.
20. Keller, C. B., Schoene, B. Samperton, K. M., *A stochastic sampling approach to zircon eruption age interpretation*. Geochemical Perspectives Letters, 2018. **8**: p. 31-35.
21. Ludwig, K. R. *ISOPLOT for MS-DOS, a plotting and regression program for radiogenic-isotope data, for IBM-PC compatible computers, version 1.00*. 1988. US Geological Survey.
22. York, D., *Least squares fitting of a straight line with correlated errors*. Earth and Planetary Science Letters, 1968. **5**: p. 320-324.
23. York, D., *Least-Squares Fitting of a Straight Line*. Canadian Journal of Physics, 1966. **44**(5): p. 1079-&.
24. York, D., Evensen, N. M., Martinez, M. L., et al., *Unified equations for the slope, intercept, and standard errors of the best straight line*. American Journal of Physics, 2004. **72**(3): p. 367-375.
25. McIntyre, G. A., Brooks, C., Compston, W., et al., *The statistical assessment of Rb-Sr isochrons*. Journal of Geophysical Research, 1966. **71**: p. 5459-5468.
26. Ludwig, K. R., *Mathematical-statistical treatment of data and errors for $^{230}\text{Th}/\text{U}$ geochronology*. Reviews in Mineralogy and Geochemistry, 2003. **52**: p. 631-656.
27. Cumming, G. L., *A recalculation of the age of the solar system*. Canadian Journal of Earth Sciences, 1969. **6**: p. 719-735.
28. Ludwig, K. R. Titterton, D. M., *Calculation of $^{230}\text{Th}/\text{U}$ isochrons, ages, and errors*. Geochimica et Cosmochimica Acta, 1994. **58**(22): p. 5031-5042.
29. James, G., Witten, D., Hastie, T., et al., *An introduction to statistical learning*. Vol. 112. 2013: Springer.
30. Smoliar, M. I., Walker, R. J. Morgan, J. W., *Re-Os ages of group IIA, IIIA, IVA, and IVB iron meteorites*. Science, 1996. **271**(5252): p. 1099-1102.
31. Selby, D., Creaser, R. A., Stein, H. J., et al., *Assessment of the ^{187}Re decay constant by cross calibration of Re-Os molybdenite and U-Pb zircon chronometers in magmatic ore systems*. Geochimica et Cosmochimica Acta, 2007. **71**(8): p. 1999-2013.

1
2
3
4
5
6
7
8
9
10
11
12
13
14
15
16
17
18
19
20
21
22
23
24
25
26
27
28
29
30
31
32
33
34
35
36
37
38
39
40
41
42
43
44
45
46
47
48
49
50
51
52
53
54
55
56
57
58
59
60

445 Table 1, Parameters for the synthetic dataset.

Age	n	initial	X	dX	Y	dY	scatter	rho
100–4500	5–30	0.2–1.2	100–1000	0.2–1%	Equation	0.2–1%	0.2–1.2%	0.4–0.999
uniform	uniform	uniform	uniform	uniform	2	uniform	uniform	uniform

446

447 Table 2, Re-Os data for the synthetic samples.

Sample No.	¹⁸⁷ Re/ ¹⁸⁸ Os	2-sigma	¹⁸⁸ Os/ ¹⁸⁸ Os	2-sigma	rho
Sample 1	100.000	1.540	1.504	0.023	0.936
Sample 2	200.000	2.940	2.407	0.024	0.473
Sample 3	300.000	4.830	3.311	0.037	0.764
Sample 4	400.000	3.960	4.215	0.078	0.565
Sample 5	500.000	7.150	5.118	0.057	0.635
Sample 6	600.000	10.200	6.022	0.090	0.484
Sample 7	700.000	11.620	6.926	0.082	0.949
Sample 8	800.000	12.880	7.830	0.078	0.945
Sample 9	900.000	12.780	8.733	0.096	0.910
Sample 10	1000.000	10.900	9.637	0.165	0.994
Sample 11	1100.000	19.580	10.541	0.065	0.477
Sample 12	1200.000	7.440	11.444	0.161	0.452

448
449

1
2
3
4
5
6
7
8
9
10
11
12
13
14
15
16
17
18
19
20
21
22
23
24
25
26
27
28
29
30
31
32
33
34
35
36
37
38
39
40
41
42
43
44
45
46
47
48
49
50
51
52
53
54
55
56
57
58
59
60

Figure 1, Data and uncertainties with associated error correlations (ρ) are presented as error ellipse and error bar (A) as well as probability density function (B). The plots show the same data and their uncertainties (cross hairs) and only vary in their correlation (values are indicated on each plot). All uncertainties are presented at the 2-sigma level (95.45% confidence).

Figure 2, The principle of the Monte Carlo based simulation is illustrated by an example comprising five samples. A) Randomly sampling a data point from the PDFs of each of the five samples and estimating its slope and y-intercept using the simple least-squares method. The slope and y-intercept from A are plotted in B. C-D) 10 and E-F) 1000 iterations of the procedure described for panels A and B. The accuracy of the final distribution (F) improves with increasing iterations / sampling.

Figure 3, The presence of model uncertainties. As illustrated by a synthetic example comprising five samples not plotting on a line, assuming no analytical uncertainties (A), sampling according to their PDFs will yield a distribution without uncertainties (B) although in fact it has uncertainty. This indicates the presence of non-analytical uncertainties, which are defined as model uncertainties and need to be accounted for. Using the same samples without analytical uncertainties (B), the model uncertainty has been illustrated by a new distribution in blue (C). A more realistic data set, in which data have analytical uncertainties (E), model uncertainties have been added to all resampled regressions, a final distribution (blue points) is obtained (F) which includes both analytical and model uncertainties.

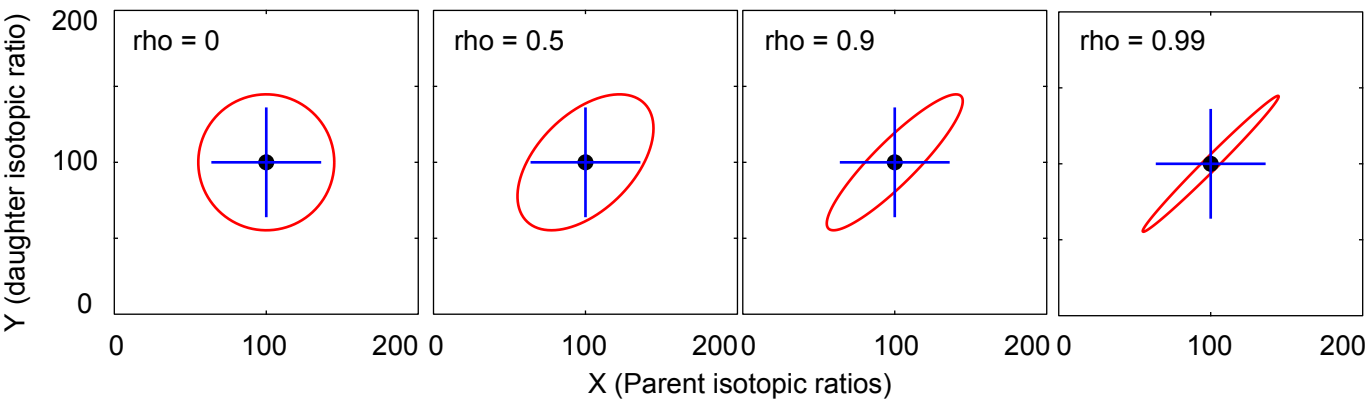
474 *Figure 4, Comparison results from Isoplot and Monte Carlo methods using synthetic examples.*

475 *Note for uncertainties from Monte Carlo method and Isoplot program, their relationship*
476 *has an abrupt change at $p=0.15$, likely due to the contrasting strategies of error*
477 *propagation in Model 1 and Model 3 solutions. Comparison of the slope estimate as a*
478 *function of the probability of fit (A) and MSWD (B) and y-intercept estimate as a function*
479 *of the probability of fit (C) and MSWD (D). The slope and y-intercept estimates, hence age*
480 *and initial isotopic ratio estimates, from the two methods are comparable. In cases when*
481 *the analytical and model uncertainties are taken into account (E, F), the uncertainties of*
482 *the slopes and y-intercepts from the Monte Carlo based simulation are larger than those*
483 *from the Isoplot program. When only the analytical uncertainties are considered (G, H),*
484 *the Isoplot Model 1 age uncertainty is comparable but slightly larger than the Monte Carlo*
485 *based approach.*

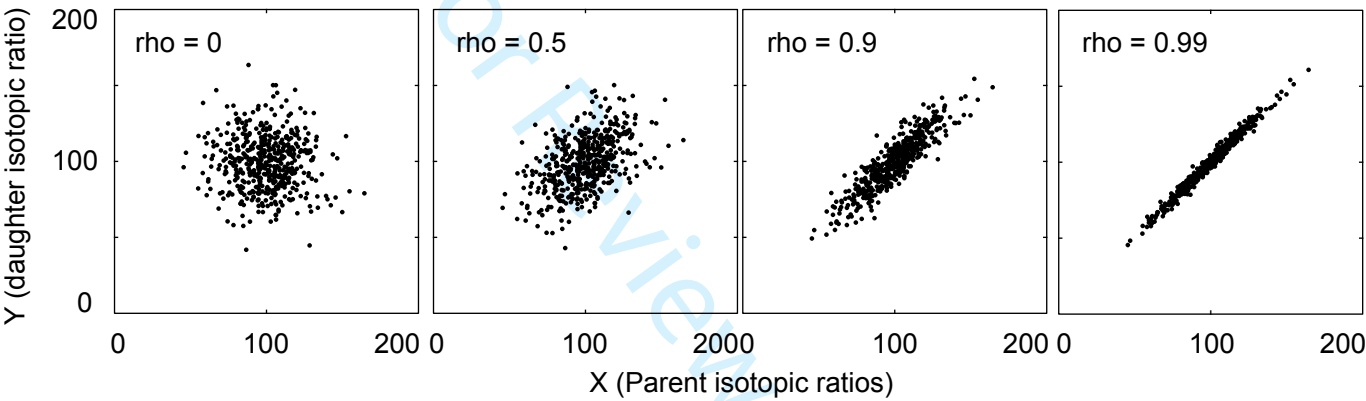
487 *Figure 5, Re-Os chronological results of the 12 synthetic samples using the Monte Carlo based*
488 *method and the Isoplot program. A), Isochron diagram using the algorithm of the Isoplot*
489 *program; B), Analytical only and analytical + model uncertainties obtained from the*
490 *Monte Carlo method at the 2-sigma level; C), The final distribution of age and initial*
491 *isotopic composition visualized by the Monte Carlo based method.*

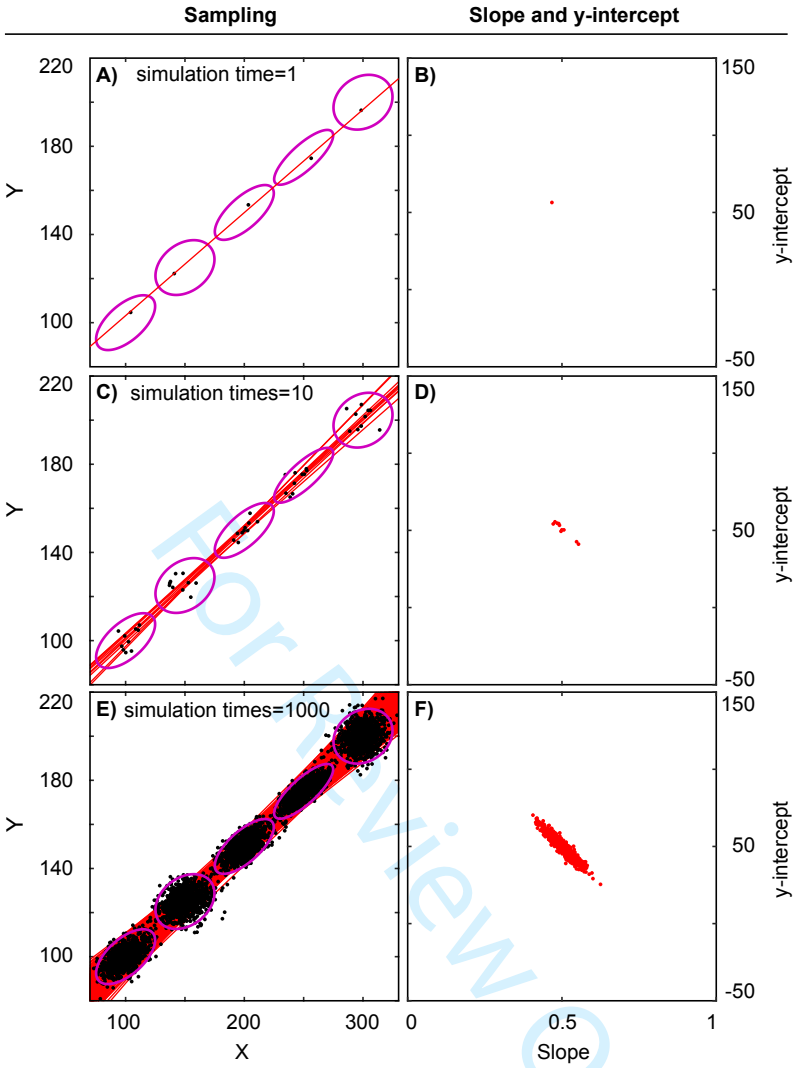
493 *Figure 6, Improving chronological constraints through integrating geological information for*
494 *the synthetic example in Figure 5. In this example, we assume that the samples are younger*
495 *than 541 Ma, and hence simulation results larger than 541 Ma are removed to yield a*
496 *better constrained chronological result.*

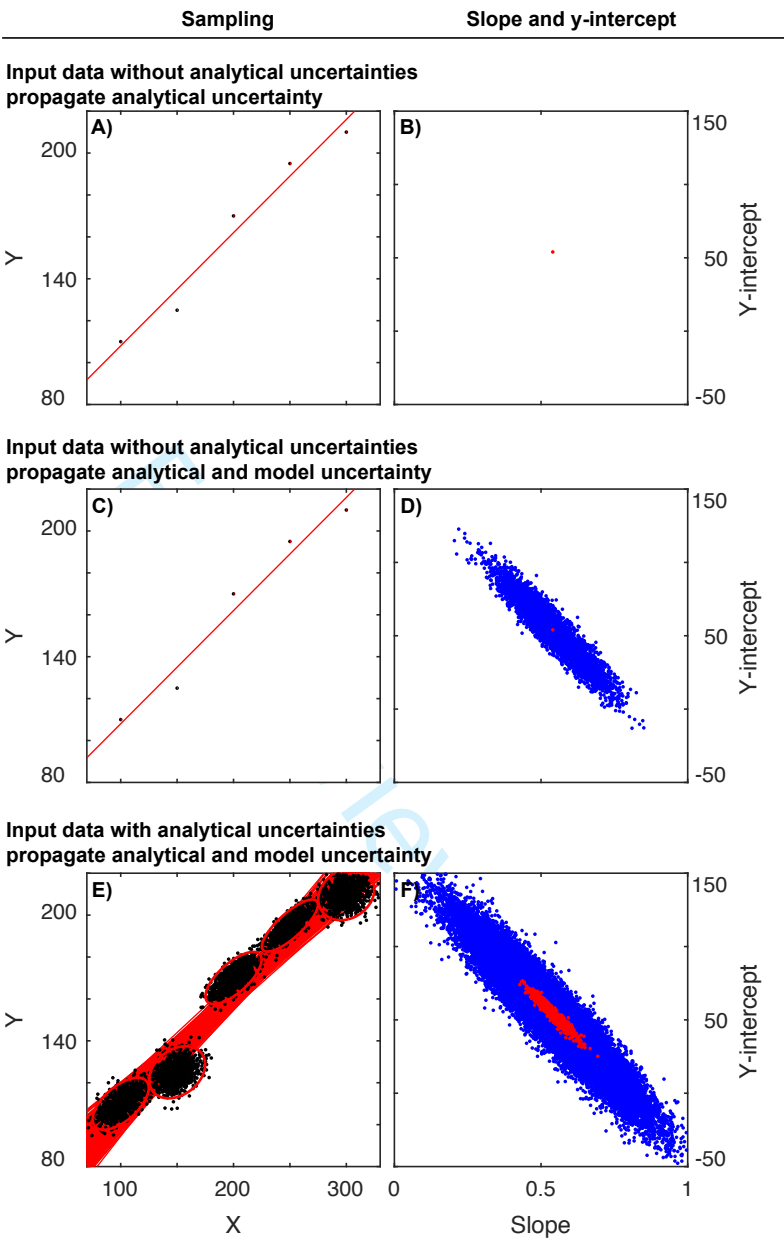
A) Error bar and error ellipse

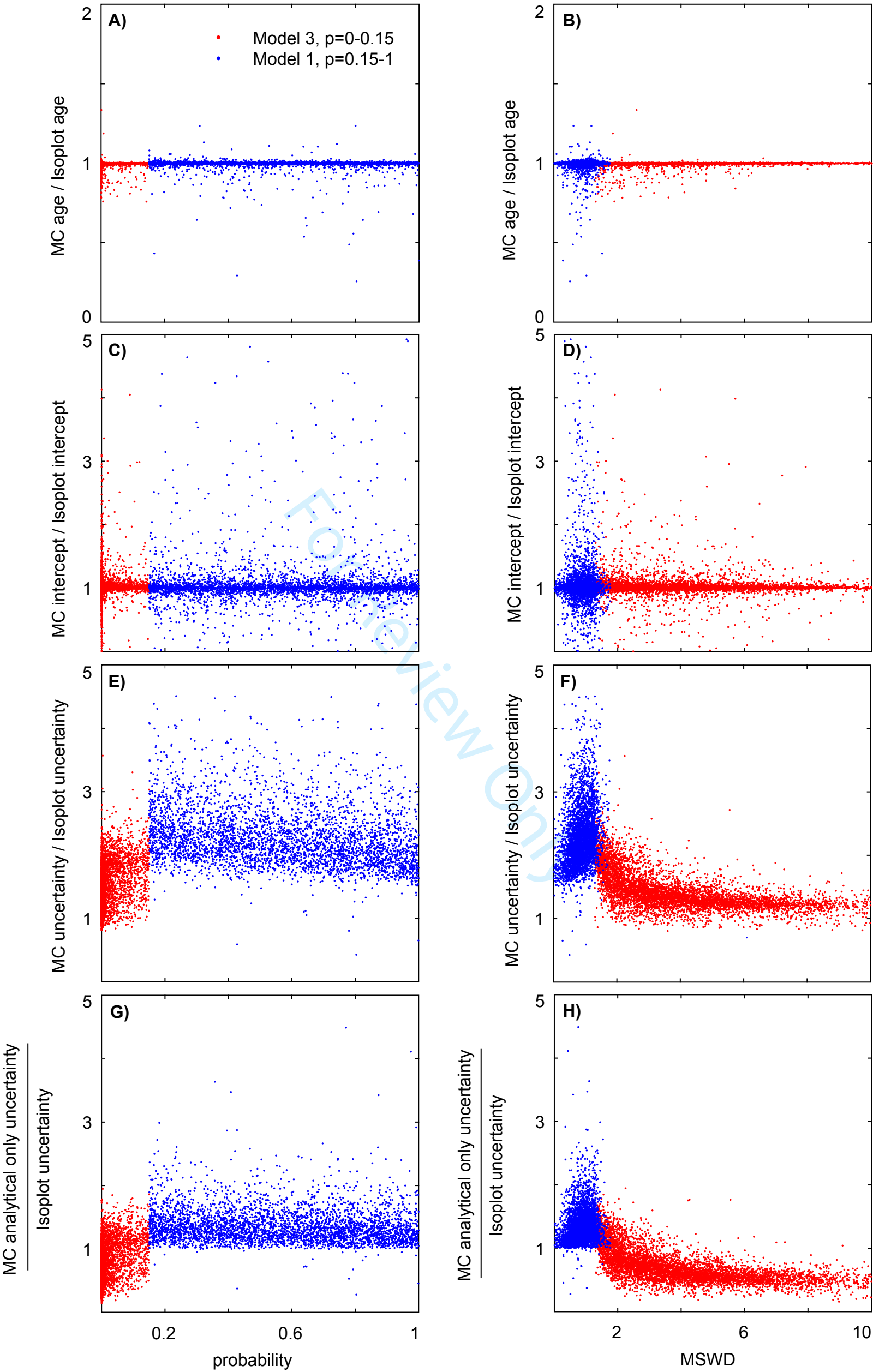


B) Probability density function

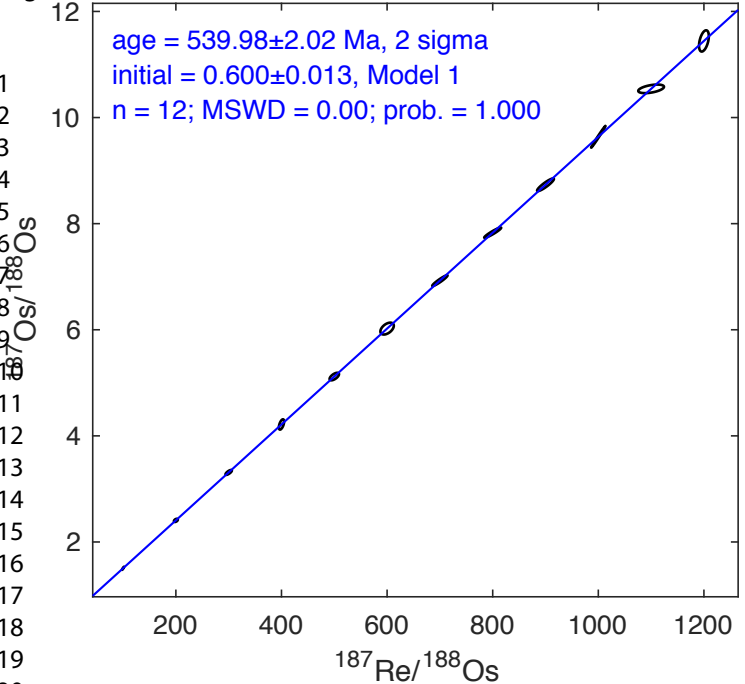




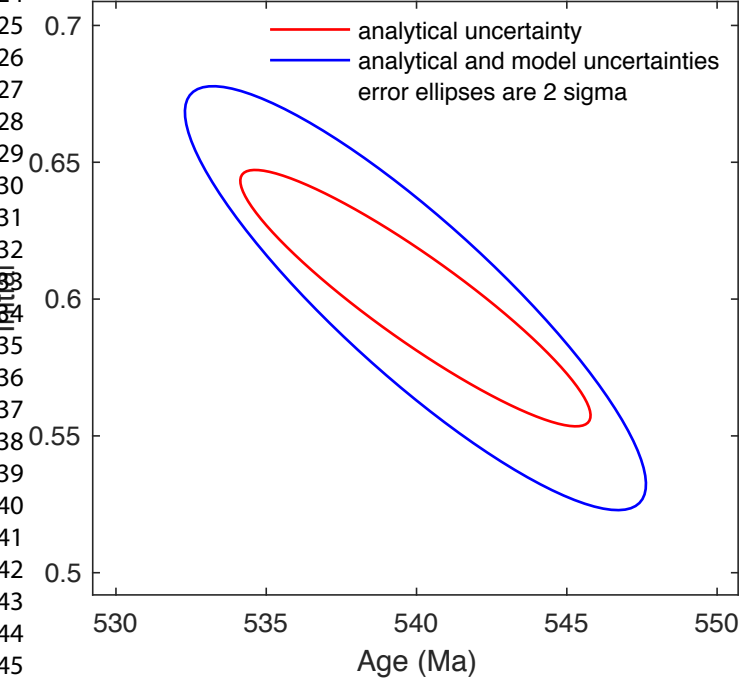




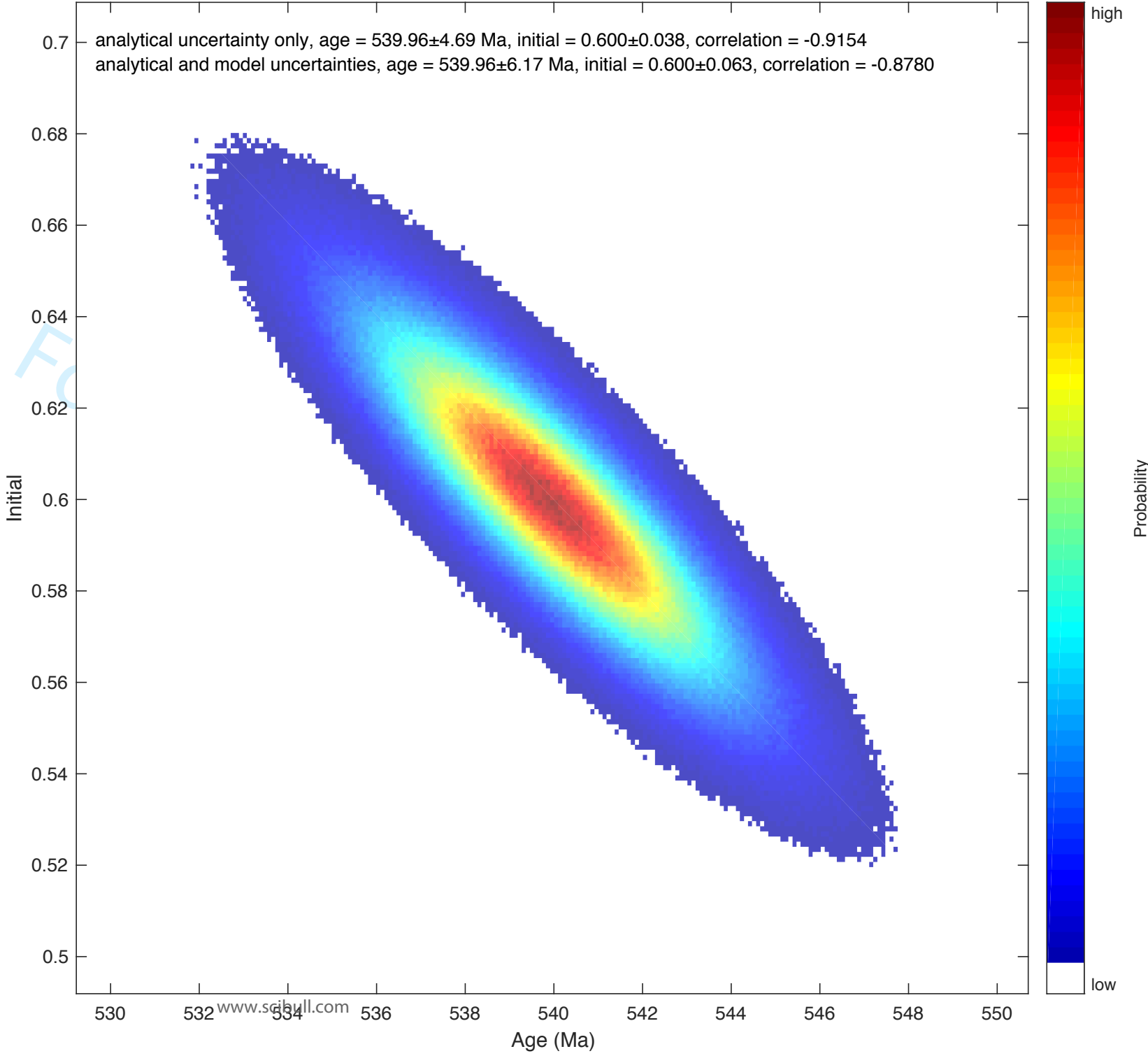
A) Ludwig Isoplot Isochron



B) Uncertainties from Monte Carlo simulation



Science Bulletin C) Contour plot of Monte Carlo simulation



C) Contour plot of Monte Carlo simulation

high

Probability

low

analytical uncertainty only, age = 539.96^{+1.92}_{-4.04} Ma, initial = 0.610^{+0.017}_{-0.035}, correlation = -0.8412
analytical and model uncertainties, age = 538.64^{+2.25}_{-5.65} Ma, initial = 0.616^{+0.026}_{-0.035}, correlation = -0.7865

www.scibull.com

Age (Ma)